

Dynamic Regulation of Quaternary Organization of the M₁ Muscarinic Receptor by Subtype-selective Antagonist Drugs*

Received for publication, December 23, 2015, and in revised form, March 29, 2016. Published, JBC Papers in Press, April 14, 2016, DOI 10.1074/jbc.M115.712562

John D. Pediani^{†1}, Richard J. Ward^{†1}, Antoine G. Godin[§], Sara Marsango[‡], and  Graeme Milligan^{‡2}

From the [†]Molecular Pharmacology Group, Institute of Molecular, Cell and Systems Biology, College of Medical, Veterinary and Life Sciences, University of Glasgow, Glasgow G12 8QQ, Scotland, United Kingdom and [§]Institut d'Optique and CNRS, Laboratoire Photonique, Numérique et Nanosciences (LP2N) and Université de Bordeaux, LP2N, F-33405, UMR 5298, 33405 Talence Cedex, France

Although rhodopsin-like G protein-coupled receptors can exist as both monomers and non-covalently associated dimers/oligomers, the steady-state proportion of each form and whether this is regulated by receptor ligands are unknown. Herein we address these topics for the M₁ muscarinic acetylcholine receptor, a key molecular target for novel cognition enhancers, by using spatial intensity distribution analysis. This method can measure fluorescent particle concentration and assess oligomerization states of proteins within defined regions of living cells. Imaging and analysis of the basolateral surface of cells expressing some 50 molecules μm^{-2} human muscarinic M₁ receptor identified a $\sim 75:25$ mixture of receptor monomers and dimers/oligomers. Both sustained and shorter term treatment with the selective M₁ antagonist pirenzepine resulted in a large shift in the distribution of receptor species to favor the dimeric/oligomeric state. Although sustained treatment with pirenzepine also resulted in marked up-regulation of the receptor, simple mass action effects were not the basis for ligand-induced stabilization of receptor dimers/oligomers. The related antagonist telenzepine also produced stabilization and enrichment of the M₁ receptor dimer population, but the receptor subtype non-selective antagonists atropine and *N*-methylscopolamine did not. In contrast, neither pirenzepine nor telenzepine altered the quaternary organization of the related M₃ muscarinic receptor. These data provide unique insights into the selective capacity of receptor ligands to promote and/or stabilize receptor dimers/oligomers and demonstrate that the dynamics of ligand regulation of the quaternary organization of G protein-coupled receptors is markedly more complex than previously appreciated. This may have major implications for receptor function and behavior.

Encoded by single polypeptides that span the plasma membrane seven times and frequently considered to be monomeric entities, it is now well established that many class A, rhodopsin family, G protein-coupled receptors (GPCRs)³ can form dimers

and/or oligomers when expressed in heterologous cell systems (1, 2). There is also growing evidence that the same may be true in native tissues (1, 2). Despite this there are many questions that remain unexplored or unresolved. These include the proportion of a receptor population that is present in such quaternary complexes, how this is affected by receptor expression level, and whether such complexes are regulated by interaction with ligands or other receptor modulators.

The family of muscarinic acetylcholine receptors, of which there are five subtypes in mammalian species (3), is a useful example to illustrate each of these issues. For example, studies on the muscarinic M₂ receptor subtype have variously concluded that it may be predominantly monomeric but with a capacity to form dimers (4), is routinely dimeric (5), or is predominantly tetrameric (6). Similar variation has been reported for each of the muscarinic M₁ (5, 7) and M₃ (8–11) subtypes. In addition, although certain studies have indicated that addition of muscarinic ligands does not affect the prevalence of receptor dimers/oligomers (5, 12), other studies have indicated a capacity for regulation. For example, the presence of muscarinic M₂ receptor homomers increased, whereas co-expressed M₂/M₃ heteromers concomitantly decreased in parallel, in an agonist-dependent manner, in cells co-expressing M₂ and M₃ receptors (13), and earlier studies had suggested that M₃ receptor homomers also either reorganized or were increased in amount in response to agonist ligands (14). These latter studies were of particular interest because the extent of the agonist-mediated effect was greatest at lower receptor expression levels and less marked at higher receptor expression levels (14). This suggests that receptor expression level may indeed play a key role and that mass action might drive dimer/oligomer production at higher receptor expression levels.

Pirenzepine (11-[(4-methylpiperazin-1-yl)acetyl]-5,11-dihydro-6*H*-pyrido[2,3-*b*][1,4]benzodiazepin-6-one) (Fig. 1) is a particularly interesting ligand in the history of muscarinic receptor pharmacology because it was the first antagonist shown to have substantially different affinity at muscarinic receptors in distinct tissues and in different regions of the central nervous system (CNS). It was thus integral in defining that there must be more than one subtype of muscarinic acetylcho-

* This work was supported by Medical Research Council Grants MR/L023806/1 and G0900050. The authors declare that they have no conflicts of interest with the contents of this article.

✂ Author's Choice—Final version free via Creative Commons CC-BY license.

[†] Both authors contributed equally to this work.

[‡] To whom correspondence should be addressed. Tel.: 44-141-330-5557; E-mail: Graeme.Milligan@glasgow.ac.uk.

³ The abbreviations used are: GPCR, G protein-coupled receptor; mEGFP, monomeric enhanced green fluorescent protein; MEU, monomeric equiv-

alent unit; NMS, *N*-methylscopolamine; P-M, palmitoylation-myristoylation; QB, quantal brightness; QNB, quinuclidinylbenzilate; ROI, region of interest; SpIDA, spatial intensity distribution analysis; Bis-Tris, 2-[bis(2-hydroxyethyl)amino]-2-(hydroxymethyl)propane-1,3-diol; hM, human M.

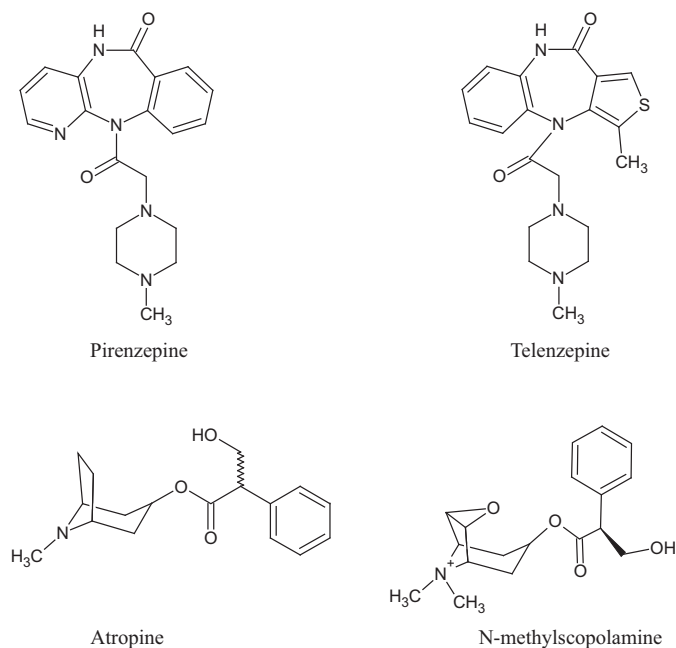


FIGURE 1. **Structures of muscarinic antagonists.** The chemical structures of pirenzepine, telenzepine, atropine, and *N*-methylscopolamine are shown.

line receptor (15), an idea subsequently confirmed by cloning of the distinct receptor subtypes (3). Pirenzepine displays substantially higher affinity for M_1 than M_2 receptors. Pirenzepine is also a medicine clinically used to treat gastric ulcers as is the closely related molecule telenzepine (4,9-dihydro-3-methyl-4-[4-methyl-1-piperazinyl]acetyl]-10*H*-thieno[3,4-*b*][1,5]benzodiazepin-10-one) (Fig. 1). These are useful medicines because their marked selectivity for the M_1 receptor subtype means that they do not significantly increase heart rate unlike the subtype non-selective, antimuscarinic drugs including atropine and *N*-methylscopolamine (Fig. 1) as this is an M_2 subtype-mediated response. Moreover, as they do not cross the blood-brain barrier effectively, they also do not inhibit M_1 -mediated cholinergic function in the CNS.

We have been exploring various approaches to define transmembrane protein organization and potential reorganization (16, 17). Herein we examine effects of pirenzepine on human M_1 receptor quaternary organization by using confocal fluorescence imaging and then subjecting such images to spatial intensity distribution analysis (SpIDA) (18–21). We show that treatment of cells induced to express the human M_1 receptor with pirenzepine dramatically increases the proportion of dimeric/oligomeric forms and that this is reversed following removal of the ligand. We also show that pirenzepine-induced dimerization is independent of a concomitant, marked increase in cell surface level of the receptor that is produced with sustained exposure to this ligand. Telenzepine, a closely related ligand that has higher affinity for the M_1 receptor than pirenzepine, produced equivalent results, but interestingly the standard subtype non-selective antagonists atropine and *N*-methylscopolamine did not. Moreover, although pirenzepine and telenzepine can also bind to the M_3 muscarinic receptor, these ligands did not produce such effects at the M_3 receptor even when used at concentrations that fully occupy this receptor subtype.

Experimental Procedures

Materials—General laboratory chemicals as well as atropine ((*RS*)-(8-methyl-8-azabicyclo[3.2.1]oct-3-yl) 3-hydroxy-2-phenylpropanoate), *N*-methylscopolamine (NMS), cytochalasin D, and both anti-tubulin antibody and secondary horseradish peroxidase-conjugated antibody were from Sigma-Aldrich or Fisher Scientific. DNA restriction endonucleases, calf intestinal alkaline phosphatase, T4 DNA polymerase, and T4 ligase were from New England Biolabs (Hitchin, UK). Wizard Plus SV Miniprep kit was from Promega (Southampton, UK). NuPAGE Novex precast 4–12% Bis-Tris gels and NuPAGE MOPS SDS running buffer were from Invitrogen. QIAfilter Plasmid Maxi kit, PCR purification kit, and QIAquick gel extraction kit were from Qiagen (Crawley, UK). Agarose was from Flowgen Biosciences (Nottingham, UK). The anti-GFP antiserum was generated in-house. ECL reagent was purchased from Pierce. [3 H]Quinuclidinylbenzilate ([3 H]QNB) and [*N*-methyl- 3 H]scopolamine methyl chloride ([3 H]NMS) were from PerkinElmer Life Sciences. Other muscarinic ligands, specifically pirenzepine and telenzepine were from Tocris (Bristol, UK). Hanks' balanced salt solution was from Life Technologies.

DNA Constructs—Enhanced green fluorescent protein incorporating an A206K mutation to reduce any tendency for the fluorescent protein to homodimerize (monomeric enhanced green fluorescent protein (mEGFP)) (22) was a gift from Dr. K. Herrick-Davis (Albany, NY). To localize mEGFP to the plasma membrane, a palmitoylation-myristoylation (P-M) sequence (23) was added to the N terminus of the fluorescent protein as described (24). h M_1 -mEGFP was also a gift from Dr. K. Herrick-Davis. h M_3 -mEGFP was made by subcloning PCR-amplified h M_3 between the *Sac*I and *Bam*HI sites of the mEGFP vector. To allow the generation of inducible Flp-InTM T-REXTM stable cell lines, these constructs were all transferred from the pEGFPN-1 plasmid (Takara Bio Europe/Clontech) backbone to pcDNA5-FRT-TO (Invitrogen). This was done by excising the appropriate region of the plasmid with *Nhe*I and *Not*I and subcloning into the pcDNA5/FRT/TO vector at *Eco*RV-*Not*I (after blunting the *Nhe*I site). All constructs were verified by sequencing.

Cell Lines—All cells were maintained in a humidified incubator with 95% air and 5% CO₂ at 37 °C. Parental Flp-In T-REX 293 cells (Invitrogen) were maintained in DMEM (high glucose) supplemented with 10% (v/v) fetal calf serum, 100 units·ml⁻¹ penicillin, 0.1 mg·ml⁻¹ streptomycin, 10 μg·ml⁻¹ blasticidin, and 100 μg·ml⁻¹ Zeocin. Cell lines generated from Flp-In T-REX 293 parental cells were maintained in DMEM (high glucose) supplemented with 10% (v/v) fetal calf serum, 100 units·ml⁻¹ penicillin, 0.1 mg·ml⁻¹ streptomycin, 10 μg·ml⁻¹ blasticidin, and 200 μg·ml⁻¹ hygromycin.

Stable Cell Line Generation—Inducible Flp-In T-REX stable cell lines able to express P-M-mEGFP, h M_1 -mEGFP, or h M_3 -mEGFP were generated as described (24). After 48 h, the medium was changed to medium supplemented with 200 μg·ml⁻¹ hygromycin to initiate selection of stably transfected cells. Pools of cells were established (10–14 days for resistant colonies to form) and tested for inducible expression by the addition of 0.1 μg·ml⁻¹ doxycycline for 48 h

Antagonist Reorganization of Muscarinic Receptor Structure

followed by screening for fluorescence corresponding to EGFP or by immunoblotting.

Cell Treatments—For antagonist treatments, cells were incubated with the appropriate concentration of compound for 16 h at 37 °C. For cytoskeletal disruption studies, cells were incubated with 2.5 $\mu\text{g}\cdot\text{ml}^{-1}$ cytochalasin D for 3 h at 37 °C.

Generation of Cell Lysates and Immunoblotting—Cells were washed once in cold phosphate-buffered saline (PBS) (120 mM NaCl, 25 mM KCl, 10 mM Na_2HPO_4 , and 3 mM KH_2PO_4 , pH 7.4) and harvested with ice-cold radioimmunoprecipitation assay buffer (50 mM HEPES, 150 mM NaCl, 1% Triton X-100, 0.5% sodium deoxycholate, 10 mM NaF, 5 mM EDTA, 10 mM NaH_2PO_4 , and 5% ethylene glycol, pH 7.4) supplemented with Complete protease inhibitor mixture (Roche Diagnostics). Extracts were passed through a 25-gauge needle and incubated for 15 min at 4 °C while on a rotating wheel. Cellular extracts were then centrifuged for 10 min at $21,000 \times g$, and the supernatant was recovered. Samples were prepared by the addition of sodium dodecyl sulfate-polyacrylamide gel electrophoresis (SDS-PAGE) sample buffer and heated to 65 °C for 5 min before being subjected to SDS-PAGE analysis using 4–12% Bis-Tris gels (NuPAGE; Invitrogen) and MOPS buffer. After separation, the proteins were electrophoretically transferred to nitrocellulose membrane, which was then blocked (5% fat-free milk powder in PBS with 0.1% Tween 20) at 4 °C on a rotating shaker overnight. The membrane was incubated for 3 h with primary antibody (1:10,000 sheep anti-GFP) in 2% fat-free milk powder in PBS-Tween, washed (3×10 min with PBS-Tween), and then incubated for 3 h with appropriate secondary antibody (horseradish peroxidase-linked rabbit anti-goat IgG diluted 1:10,000 in 2% fat-free milk powder in PBS-Tween). After washing as above, proteins were detected by enhanced chemiluminescence (Pierce Chemical) according to the manufacturer's instructions.

Cell Membrane Preparations—Cells induced with the required concentration of doxycycline to express hM_1 -mEGFP or hM_3 -mEGFP were washed and then harvested with ice-cold PBS. Pellets of cells were frozen at -80 °C for a minimum of 1 h, thawed, and resuspended in ice-cold 10 mM Tris and 0.1 mM EDTA, pH 7.4 (TE buffer) supplemented with Complete protease inhibitor mixture. Cells were homogenized on ice by 40 strokes of a glass-on-Teflon homogenizer followed by centrifugation at $1000 \times g$ for 5 min at 4 °C to remove unbroken cells and nuclei. The supernatant fraction was removed and passed through a 25-gauge needle 10 times before being transferred to ultracentrifuge tubes and subjected to centrifugation at $90,000 \times g$ for 30 min at 4 °C. The resulting pellets were resuspended in ice-cold TE buffer. Protein concentration was assessed, and membranes were stored at -80 °C until required.

[^3H]QNB Binding Assays—Both single concentration binding studies and saturation binding curves were established by the addition of 20 μg of membrane protein to assay buffer (20 mM HEPES, 100 mM NaCl, and 10 mM MgCl_2 , pH 7.5) containing either a single, near saturating concentration (5 nM), or varying concentrations of [^3H]QNB (0.01–30 nM). Nonspecific binding was determined in the presence of 10 μM atropine. Reactions were incubated for 120 min at 30 °C, and bound ligand was separated from free by vacuum filtration through GF/C filters

(Brandel Inc., Gaithersburg, MD) that had been presoaked in assay buffer. The filters were washed twice with cold assay buffer, and bound ligand was estimated by liquid scintillation spectrometry. Competition binding assays were carried out in a similar way but with a constant concentration of [^3H]QNB (1 nM) and the addition of a range of concentrations of ligands of interest (0.03 nM–1 mM). Data were analyzed using GraphPad Prism 5.03 (GraphPad Software, La Jolla, CA).

[^3H]NMS Binding Assay—Flp-In T-REx 293 cells able to express a construct of interest were grown overnight on white 96-well microtiter plates that had been treated with 0.1 $\text{mg}\cdot\text{ml}^{-1}$ poly-D-lysine. Cells were then treated with various concentrations of doxycycline for 24 h at 37 °C. The medium was removed and replaced with 100 μl /well cold PBS containing 1 nM [^3H]NMS. Nonspecific binding was determined in the presence of 10 μM atropine. The plates were incubated at 4 °C for 150 min, and the assay was terminated by removal of the binding mixture followed by washing with 4×100 μl /well ice-cold PBS. One hundred microliters/well Microscint 20 (PerkinElmer Life Sciences) was added, and the plates were sealed before overnight incubation at room temperature on a rapidly shaking platform. Bound ligand was determined using a Packard Topcount NXT (PerkinElmer Life Sciences). Using the specific binding per well and number of cells per well, the receptor copies per cell was determined.

Inositol Monophosphate Assay—Inositol monophosphate accumulation assays were performed using Flp-In T-REx 293 cells able to express the hM_3 -mEGFP receptor construct in an inducible manner. Experiments were performed using a homogenous time-resolved FRET-based detection kit (CisBio Bioassays, Codolet, France) according to the manufacturer's protocol. Cells were plated at 7500 cells/well in low volume 384-well plates, and the ability of various concentrations of the agonist carbachol to increase the level of inositol monophosphate was assessed following incubation for 2 h with the agonist. In appropriate experiments, this was preceded by a 15-min preincubation with the indicated concentrations of antagonist (atropine, pirenzepine, or telenzepine).

Monitoring of mEGFP Fluorescence Emission Spectrum—Flp-In T-REx 293 cell lines able to express hM_1 -mEGFP were grown to 100,000 cells/well in 96-well solid black bottom plates (Greiner Bio-One) precoated with 0.1 $\text{mg}\cdot\text{ml}^{-1}$ poly-D-lysine. Cells were treated with 100 $\text{ng}\cdot\text{ml}^{-1}$ doxycycline to induce the expression of hM_1 -mEGFP. After 24-h induction, cells were washed three times in Hanks' balanced salt solution buffer. 100 μl of Hanks' balanced salt solution was added to each well, and the plates were read using a CLARIOstar fluorescence plate reader (BMG Labtechnologies). Specifically, cells were excited at 462 nm, and the emission spectrum between 500 and 600 nm was collected at 5-nm intervals. The same process was repeated after the addition to each well of 100 μl of Hanks' balanced salt solution supplemented with the vehicle or the appropriate muscarinic receptor antagonist.

SpIDA—SpIDA was carried out essentially as described (24). All region of interest (RoI) measurements were selected from the basolateral membrane surface. Monomeric equivalent unit (MEU) values for hM_1 -mEGFP or hM_3 -mEGFP were measured by normalizing their quantified quantal brightness (QB) values

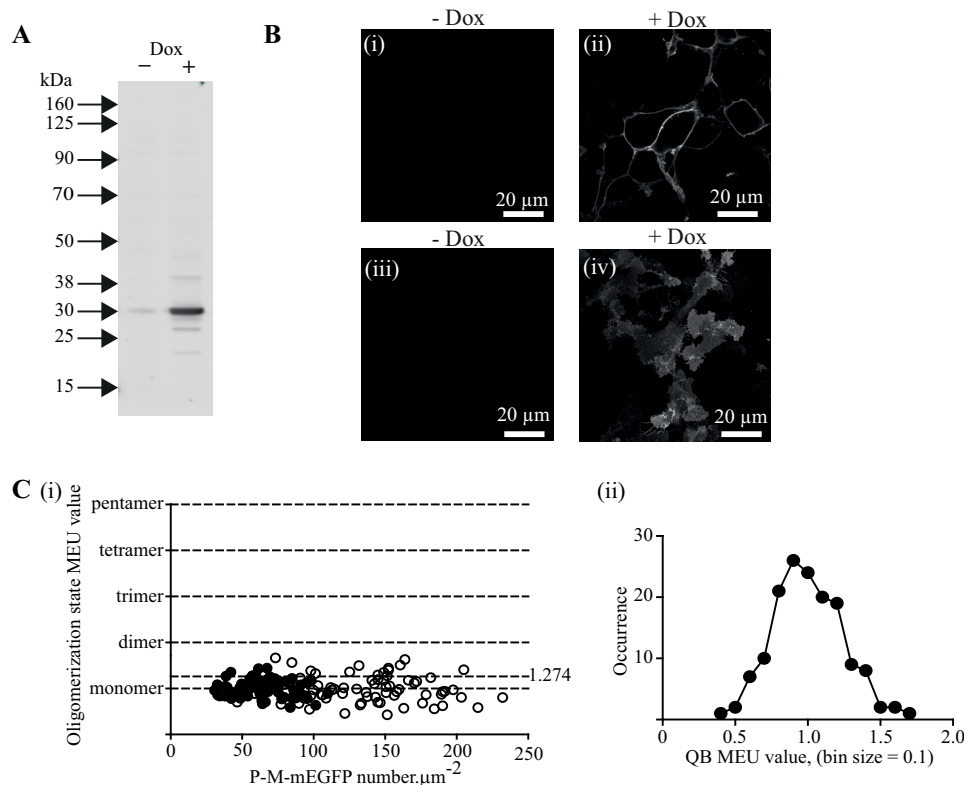


FIGURE 2. Expression, cellular distribution profile, and quantal brightness analysis of plasma membrane-targeted mEGFP. Flp-In T-REx 293 cells harboring P-M-mEGFP were maintained in the absence of doxycycline ($-Dox$) or treated with doxycycline ($10 \text{ ng}\cdot\text{ml}^{-1}$) for 24 h ($+Dox$). Lysates of these cells were resolved by SDS-PAGE and immunoblotted with an anti-GFP antiserum (A). In B, images of uninduced cells (panels *i* and *iii*) or cells induced to express P-M-mEGFP (panels *ii* and *iv*) are shown. B, panels *i* and *ii*, confocal images across groups of cells. B, panels *iii* and *iv*, images of the basolateral surface of such cells. C, panel *i*, shows QB assessed in individual Rols (presented as monomeric equivalent units) plotted against number of $\text{mEGFP}\cdot\mu\text{m}^{-2}$ of the basolateral surface. Filled symbols, cells treated with $2.5 \text{ ng}\cdot\text{ml}^{-1}$ doxycycline; open symbols, cells treated with $10 \text{ ng}\cdot\text{ml}^{-1}$ doxycycline. C, panel *ii*, QB values from individual Rols were binned (bin size, 0.1 MEU), and these displayed a symmetrical distribution (see “Results”).

to average QB values measured from the P-M-mEGFP construct using exactly the same laser power as used to excite the muscarinic receptor subtype constructs. To distinguish between monomeric and dimeric/oligomeric hM_1 -mEGFP or hM_3 -mEGFP species, P-M-mEGFP MEU occurrence/frequency x - y graphs (MEU bin size = 0.1) were plotted for each MEU value measured during excitation with laser power set to 2 or 6%. Such plots revealed a symmetrical distribution of the values, and GraphPad Prism normality tests indicated the distributions were Gaussian (see “Results” and “Statistical Analyses”). The data from each frequency x - y plot measured using 2 or 6% laser power were combined as this range of excitation settings was required to illuminate the muscarinic receptor subtypes optimally at differing expression levels without erroneous detector pixel saturation occurring. From this combined plot, an MEU value of 1.274 (which represented 75% of the data set, falling within the mean ± 1.5 standard deviations) was set as a border to distinguish between monomeric and larger complexes in studies where individual MEU values exceeded 1.274. The distribution of such values for the muscarinic receptor constructs was non-Gaussian and skewed toward higher values.

Calculation of Receptor Density at the Cell Surface by SpIDA—SpIDA software also reports the mean fluorescence intensity for each ROI analyzed. The number of hM_1 -mEGFP, hM_3 -mEGFP, or P-M-mEGFP molecules/ μm^{-2} (density) was

measured by dividing the mean fluorescence intensity value by the quantified monomeric QB value.

Statistical Analyses—Variation in receptor number or mean/median of QB produced by treatment with either ligands or varying concentrations of doxycycline was assessed by one-way analysis of variance with the use of Bonferroni’s or Dunnett’s test for multiple comparisons as appropriate. Normality distributions of recovered QB values defined as MEUs were assessed by each of D’Agostino and Pearson, Kolmogorov-Smirnov, and Shapiro and Wilk normality tests (at $p > 0.05$) and by skewness and Kurtosis assessments. Distributions that failed any of the three normality assessments (at $p < 0.05$) were considered to be non-Gaussian.

Results

A cDNA encoding A206K mEGFP that incorporated an N-terminal addition of a plasma membrane-targeting P-M sequence was cloned into the doxycycline-inducible Flp-In T-REx locus of Flp-In T-REx 293 cells. Following addition of doxycycline ($10 \text{ ng}\cdot\text{ml}^{-1}$) to these cells, a polypeptide of the anticipated molecular mass (30 kDa) was identified by immunoblotting SDS-PAGE-resolved cell lysates with an anti-GFP antiserum (Fig. 2A). Confocal imaging of the cells confirmed plasma membrane targeting of the P-M-mEGFP construct following addition of doxycycline (Fig. 2B, panels *i* and *ii*). Imaging

Antagonist Reorganization of Muscarinic Receptor Structure

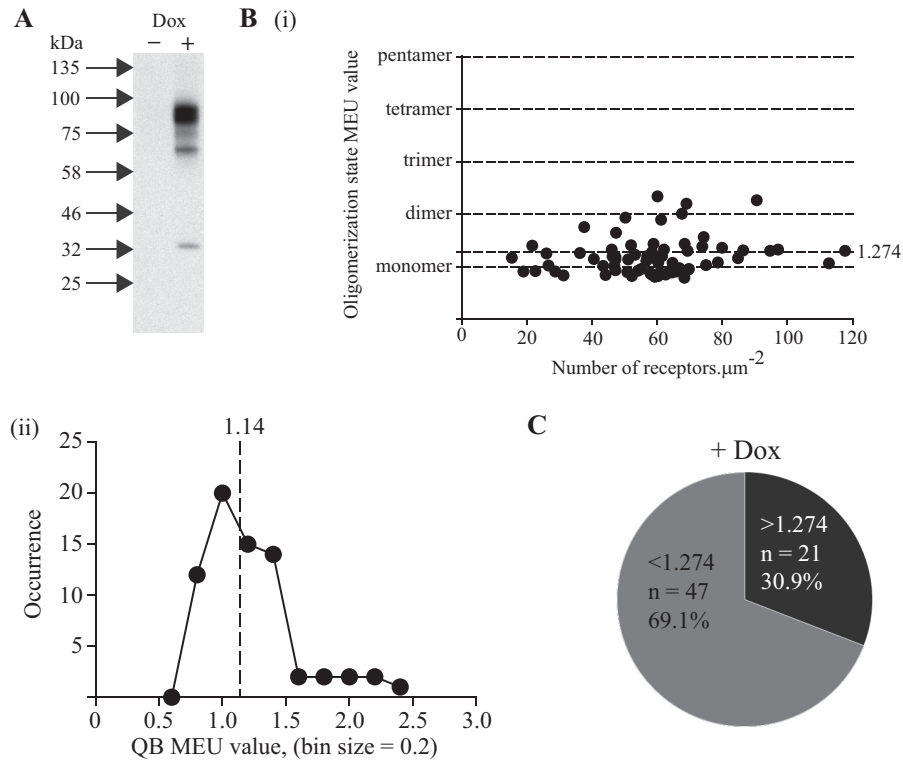


FIGURE 3. hM₁-mEGFP exists as a mixture of monomers and oligomers in the basal state. Flp-In T-Rex 293 cells harboring hM₁-mEGFP were maintained in the absence of doxycycline (– Dox) or treated with doxycycline (100 ng·ml^{–1}) for 24 h (+ Dox). Lysates of these cells were resolved by SDS-PAGE and immunoblotted with an anti-GFP antiserum (A). B, panel i, shows QB detected in individual RoIs (presented as monomeric equivalent units) plotted against number of hM₁-mEGFP·μm^{–2} of the basolateral surface (55.7 ± 2.3 μm^{–2}, mean ± S.E., n = 68). B, panel ii, QB values from individual RoIs were binned (bin size, 0.2 MEU). These displayed a non-symmetrical distribution skewed to values >1.00 MEU. Dotted line, median value. C, in this data set, 47 of the 68 measurements were assessed as being predominantly monomeric (69.1%).

RoIs of the basolateral membrane of these cells (Fig. 2B, panels *iii* and *iv*) and subsequent analysis of such images by SpIDA (18, 19, 21, 24, 25) indicated that, with laser power set to 2%, this polypeptide displayed QB of 12.15 ± 0.39 units (mean ± S.E., n = 76). Based on fluorescence intensity measurements, in this set of studies the average expression level of P-M-mEGFP within the basolateral membrane was 133.8 ± 4.7 molecules·μm^{–2} (mean ± S.E., n = 76) and in individual RoIs this ranged between 46 and 232 molecules·μm^{–2} (Fig. 2C, panel *i*). Variation in the concentration of doxycycline used can allow control of the level of expression of the polypeptide harbored at the Flp-In T-REX locus of such cells. Following treatment of these cells with 2.5 ng·ml^{–1} doxycycline, levels of expression of P-M-mEGFP were lower, and appropriate analysis of confocal images taken from the cells required laser power to be increased. With laser power set to 6%, the P-M-mEGFP polypeptide displayed QB of 25.24 ± 0.54 (mean ± S.E., n = 76) with an average expression level of 62.1 ± 2.2 molecules·μm^{–2}. In individual RoIs, this ranged between 1 and 109 molecules·μm^{–2} (Fig. 2C, panel *i*).

To assess whether P-M-mEGFP was detected as monomeric across the full expression range achieved, we combined these two data sets. This resulted in an average expression level of 99.0 ± 3.9 molecules·μm^{–2} (mean ± S.E., n = 152). Information from each individual RoI was plotted as multiples of the average QB, *i.e.* 12.15 or 25.24, respectively, for those obtained with laser power set to 2 or 6%, and defined as MEU (Fig. 2C, panel *i*). Analysis of this combined data set showed it to be

consistent with Gaussian distribution, and as such there was no evidence to suggest that at higher levels of expression proximity of individual molecules of P-M-mEGFP resulted in incorrect assignment of these as being non-monomeric (Fig. 2C, panel *ii*). Based on the distribution of values of MEU for P-M-linked mEGFP that represented 75% of the data set, falling within the mean ± 1.5 S.D., in subsequent studies we defined QB values ≤1.274 MEU as being monomeric, whereas QB values >1.274 MEU were regarded as reflecting complexes that were larger than monomers (Fig. 2C, panel *ii*) (see “Experimental Procedures” for further details).

We next generated equivalent Flp-In T-REX 293 cells in which cDNA encoding a form of the human M₁ muscarinic receptor with C-terminally fused mEGFP (hM₁-mEGFP) was cloned into the Flp-In T-REX locus. Once more this allowed expression of the receptor construct only upon addition of doxycycline with maximal expression obtained by use of 100 ng·ml^{–1} doxycycline. The receptor was detected as a single species, of apparent molecular mass close to 80 kDa, by immunoblotting lysates of untreated and doxycycline-treated cells following resolution by SDS-PAGE (Fig. 3A). Fluorescence intensity measurements of RoI from the basolateral membrane of these cells indicated hM₁-mEGFP to be expressed at 58.3 ± 2.4 copies·μm^{–2} (n = 68) but with extremes of variation across these RoIs of greater than 4-fold (Fig. 3B, panel *i*). SpIDA of the images from these RoI, assessed at 2% laser power, indicated a median QB of 13.85 units (n = 68). This corresponds to 1.14 MEU (*i.e.* 1.14 MEU times the mean value of the monomeric

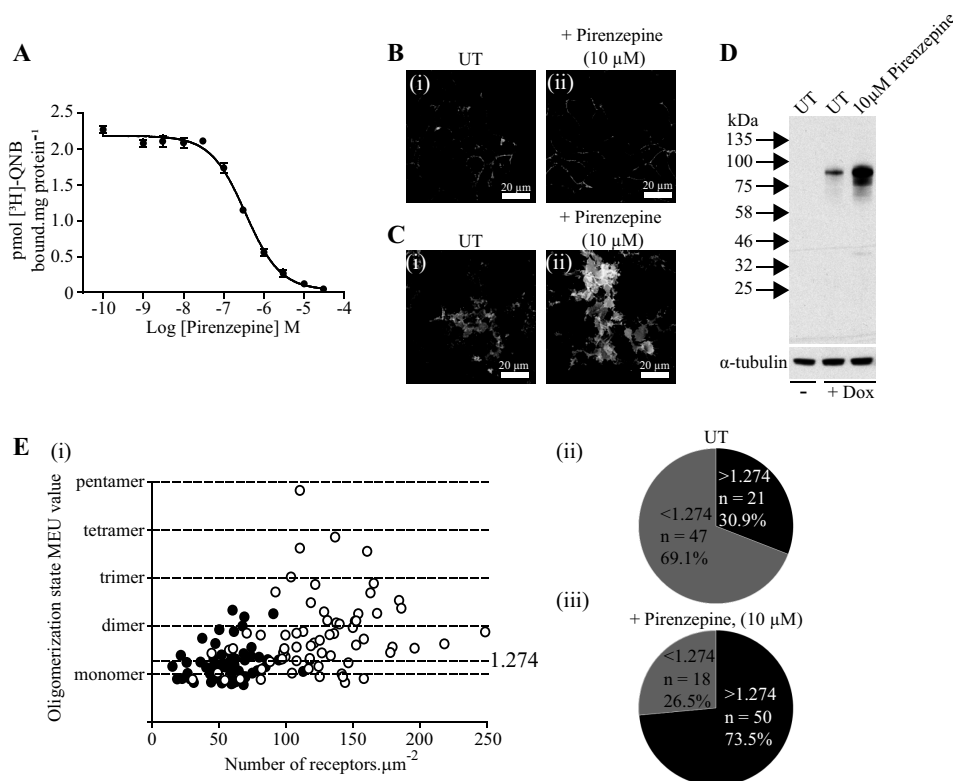


FIGURE 4. Sustained treatment with pirenzepine causes relocation and up-regulation of hM₁-mEGFP and promotes oligomerization of the receptor. Flp-In T-REx 293 cells harboring hM₁-mEGFP were treated with doxycycline (100 ng·ml⁻¹) for 24 h. *A*, membrane preparations from these cells were used in ligand binding studies using 1 nM [³H]QNB and varying concentrations of pirenzepine. Based on the K_d for [³H]QNB, estimated as 98 ± 17 pM, the inhibition constant (pK_i) for pirenzepine was calculated as 7.66 ± 0.04 . Shown is a representative graph from $n = 3$; error bars represent \pm S.E. Cells were then treated with vehicle (UT) or with pirenzepine (10 μM) for 24 h. *B*, panels *i* and *ii*, confocal images as in Fig. 2 showed that treatment with pirenzepine resulted in relocation of hM₁-mEGFP to enhance cell surface/plasma membrane localization. *C*, panels *i* and *ii*, imaging the basolateral surface of a group of cells indicated that pirenzepine caused up-regulation of hM₁-mEGFP. *D*, immunoblotting studies confirmed that pirenzepine caused up-regulation of hM₁-mEGFP. α-Tubulin acted as a loading control. *E*, panels *i*–*iii*, quantal brightness and fluorescence intensity analysis from SpIDA confirmed an overall 2.1-fold up-regulation of receptor number at the basolateral surface and that a substantially greater proportion of the RoIs were identified as containing dominantly receptor dimers/oligomers (73.5%) following pirenzepine treatment (*open symbols*) than in vehicle-treated controls (30.9%) (*filled symbols*).

P-M-linked mEGFP). Here, however, distribution of the individual observations was non-Gaussian with skew toward higher values (Fig. 3*B*, panel *ii*). This is consistent with, at this expression level, the majority of the receptor construct being monomeric but with a proportion being within larger quaternary structures, *i.e.* dimeric and/or oligomeric. The percentage of hM₁-mEGFP RoI QB values defined as “larger than monomer” in this data set was 30.9% (Fig. 3*C*). Although very modest ($r^2 = 0.032$), over this limited range of expression levels, there was a positive correlation between receptor number and the presence of non-monomeric species observed in distinct RoIs (see later). Although the number of observations in this specific data set was restricted to 68, subsequently, at the completion of the experimental studies, we combined the full data sets generated for cells induced to express hM₁-mEGFP but not further treated ($n = 478$). Analysis confirmed the non-Gaussian distribution of the QB corresponding to hM₁-mEGFP and allowed estimation of the percentage of RoI QB values that were consistent with the mean basal receptor being larger than monomer as 25.7%.

Pirenzepine (15) is the prototypic M₁-selective muscarinic receptor antagonist and has been reported to stabilize dimers of this receptor (26). Competition binding experiments between pirenzepine and the muscarinic antagonist [³H]QNB ($K_d = 98 \pm 17$ pM) allowed definition of the affinity of pirenzepine

($pK_i = 7.66 \pm 0.04$) for the hM₁-mEGFP construct (Fig. 4*A*). Initially Flp-In T-REx 293 cells induced to express hM₁-mEGFP by treatment with 100 ng·ml⁻¹ doxycycline were incubated for 16 h with vehicle or with a single concentration of pirenzepine (10 μM) calculated to be sufficient to occupy greater than 99% of the receptor population. Imaging of these vehicle- and pirenzepine-treated cells illustrated a number of features. First, confocal images across the center of the cells showed that, as with many GPCRs, although a substantial proportion of the hM₁ receptor construct was located at the plasma membrane in vehicle-treated cells, a significant fraction was inside the cells and located within punctate vesicles (Fig. 4*B*, panel *i*). By contrast, following treatment with pirenzepine very little of the receptor was detected within the cells, and the construct was highly concentrated at the cell surface (Fig. 4*B*, panel *ii*). Imaging of the basolateral surface of groups of these cells indicated that there was marked up-regulation of hM₁-mEGFP following such sustained treatment with pirenzepine (Fig. 4*C*), and this was confirmed in immunoblotting studies (Fig. 4*D*). Fluorescence intensity of RoI and associated SpIDA within the basolateral membrane of such pirenzepine-treated cells indicated that at 2% laser power the median QB of the receptor construct (19.50 units, $n = 68$, *i.e.* 1.61 MEU) increased markedly ($p < 0.001$) compared with the untreated cells (Fig. 4*E*). This was

Antagonist Reorganization of Muscarinic Receptor Structure

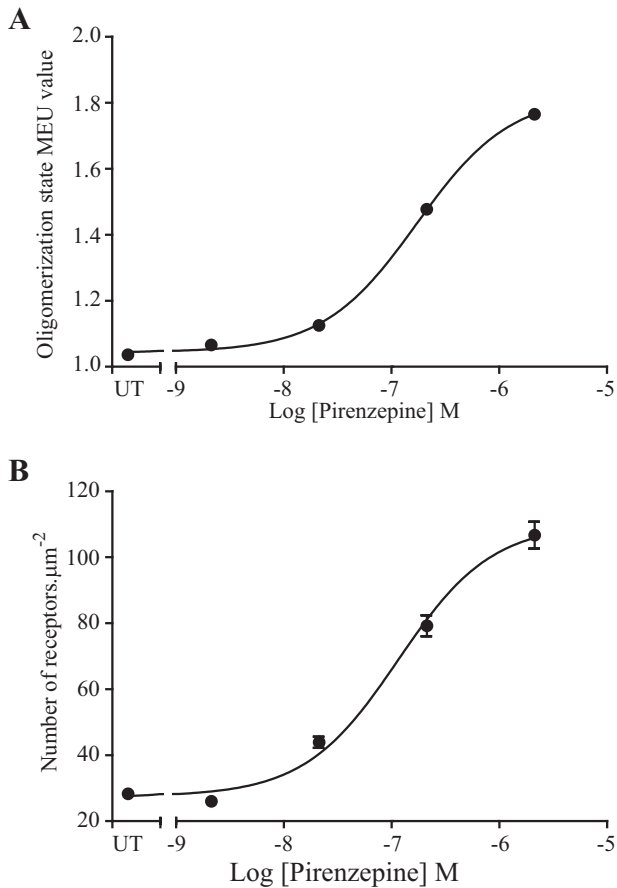


FIGURE 5. Pirenzepine-induced increases in both receptor oligomerization and expression levels are concentration-dependent. Experiments akin to those of Fig. 4 were performed on Flp-In T-REx 293 cells harboring hM₁-mEGFP that had been treated with doxycycline (100 ng·ml⁻¹) for 24 h and then treated with the indicated concentrations of pirenzepine. QB values corresponding to hM₁-mEGFP were plotted as monomeric equivalent units against pirenzepine concentration (A) as were the number of receptor molecules·μm⁻² (B). Data are presented as median (A) and mean (B). Error bars represent ±S.E.; *n* = 84 in each case. UT, untreated.

consistent with a substantial increase (to 73.5%) in the percentage of RoI containing predominantly dimeric/oligomeric complexes (Fig. 4E). Indeed, examination of the individual observations from distinct RoIs indicated a significant proportion of these to be potentially consistent with the receptor existing in complexes that were larger than dimers (Fig. 4E). Notably, the effect of pirenzepine to both enhance QB of hM₁-mEGFP (Fig. 5A) and increase the number of copies of the receptor construct (Fig. 5B) was concentration-dependent with half-maximal effect produced by close to 100 nM ligand.

Although the oligomeric organization of hM₁-mEGFP was clearly more complex after sustained treatment of the cells with pirenzepine, the correlation between receptor expression levels and receptor quaternary complexity was now also markedly increased ($r^2 = 0.22$) compared with the untreated cells. However, we have shown previously that dimeric and oligomeric organization of another class A GPCR, the serotonin 5-HT_{2C} receptor, increases simply with expression level of the receptor (24). Therefore, because basolateral membrane receptor number was increased on average to 122.4 ± 5.1 copies·μm⁻² following sustained pirenzepine treatment (Fig. 4D), it was im-

possible from these initial studies to determine whether pirenzepine directly promoted and/or stabilized dimeric/oligomeric forms of the hM₁ receptor or whether receptor up-regulation produced at the basolateral surface of the cells by treatment with this antagonist ligand was sufficient by itself to account for these observations. A specific feature of the Flp-In T-REx locus is that the level of expression of polypeptides can be controlled by varying the concentration of doxycycline used (27). We, therefore, treated cells harboring hM₁-mEGFP at this locus with a range of concentrations of doxycycline for 24 h. Immunoblotting SDS-PAGE-resolved lysates from these cells with the anti-GFP antiserum showed variation in expression of the receptor over the range 1–100 ng·ml⁻¹ doxycycline (Fig. 6A). In parallel, binding of a near saturating concentration of [³H]QNB to membrane preparations of these cells provided confirmation that the increasing immunological identification of the receptor with doxycycline concentration was indeed consistent with increasing numbers of receptors that could bind the muscarinic antagonist (Fig. 6B). Based on these results, we selected to study organization of hM₁-mEGFP in cells treated with 2.5 ng·ml⁻¹ doxycycline. In such cells, analysis of basolateral RoIs confirmed that receptor expression was reduced (14.4 ± 0.7 receptors·μm⁻²) compared with those treated with the maximally effective concentration of doxycycline (Fig. 6C). Although this level was significantly lower ($p < 0.001$) than the 58.3 ± 2.4 copies·μm⁻² recorded earlier in cells treated with 100 ng·ml⁻¹ doxycycline, this did not result in a significant alteration in average QB and indicated that in both situations the majority of the receptors were monomeric (Fig. 6C). Now, although overnight treatment with pirenzepine (10 μM) once more significantly increased ($p < 0.001$) receptor density (now to 54.5 ± 1.9 copies·μm⁻², *n* = 70) at the basolateral membrane (Fig. 6C), it did so only to the same levels as present in cells induced with 100 ng·ml⁻¹ doxycycline but not treated with pirenzepine (*i.e.* 58.3 ± 2.4 copies·μm⁻²). QB and SpIDA assessment now indicated that, at the same level of basolateral cell surface expression of hM₁-mEGFP, pirenzepine treatment had indeed produced a substantial increase in overall receptor complex organization as MEU increased to 1.73 (median). In these experiments, following pirenzepine treatment the vast majority of the RoIs (91.4%) had a higher average receptor oligomerization state than the monomer (*e.g.* dimeric/oligomeric), whereas without pirenzepine treatment only in 30% of the RoIs were there receptors that were not largely monomeric (Fig. 6D).

We next considered whether shorter term treatment with pirenzepine would also result in receptor dimerization/oligomerization without causing the potentially confounding degree of receptor up-regulation. For these studies, we used cells that in the absence of pirenzepine had been induced to express the receptor by treatment with 100 ng·ml⁻¹ doxycycline. In this set of studies, analysis of RoI from the basolateral surface quantified the hM₁-mEGFP receptor construct to be present at 41.8 ± 1.3 copies·μm⁻² (*n* = 134) with a median MEU of 1.12 (Fig. 7A). SpIDA indicated that in 26.9% of the RoI receptors were present dominantly within dimeric/oligomeric complexes. Treatment of the cells with pirenzepine (10 μM) for 90 min did result in a small increase ($p < 0.01$) in overall basolateral receptor density to 54.1 ± 1.7 copies·μm⁻² (*n* = 134) (Fig. 7A). However,

Antagonist Reorganization of Muscarinic Receptor Structure

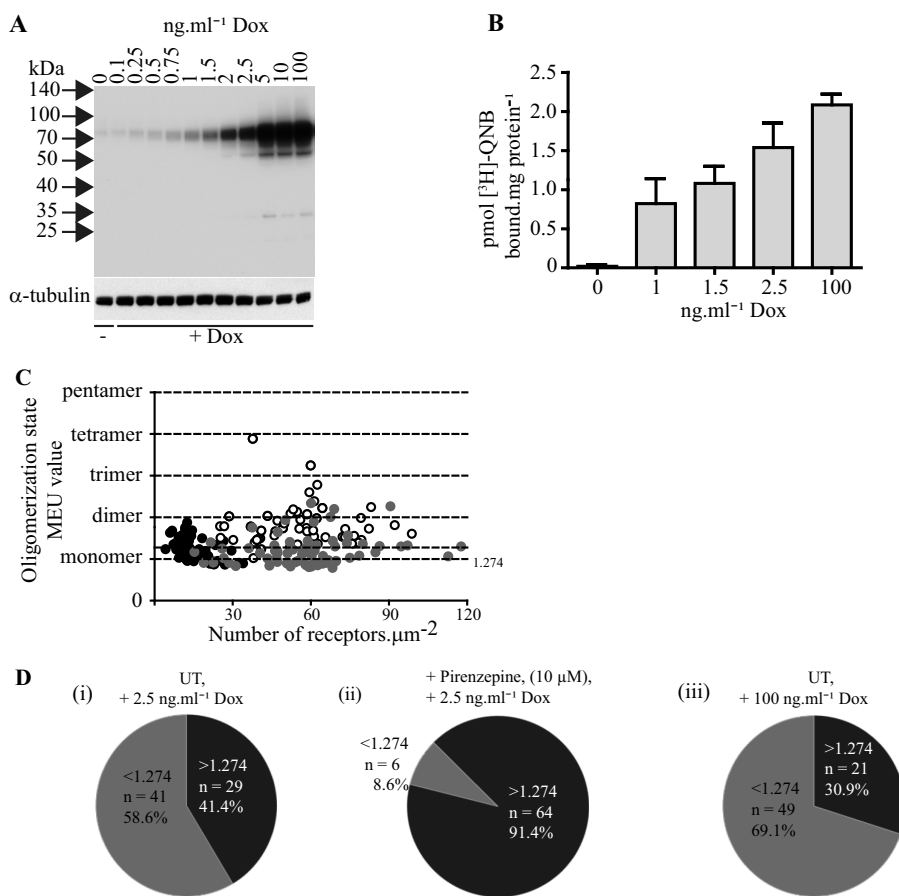


FIGURE 6. Pirenzepine stabilizes hM₁-mEGFP dimers/oligomers independently from effects on receptor expression levels. Flp-In T-Rex 293 cells harboring hM₁-mEGFP were treated with varying concentrations of doxycycline (*Dox*). *A*, lysates from these cells were immunoblotted with an anti-GFP antiserum to assess relative expression levels of the receptor construct. α -Tubulin acted as a loading control. *B*, specific binding of a single near receptor saturating concentration of [³H]QNB (5 nM) was assessed in cell membrane preparations generated from cells treated with the indicated concentrations of doxycycline. Shown are combined data from $n = 3$ experiments; *error bars* represent \pm S.E. *C*, comparisons of QB (presented as monomeric equivalent units) and receptor expression levels in cells induced to express hM₁-mEGFP by treatment with 2.5 ng·ml⁻¹ doxycycline (*black symbols*), treatment with 100 ng·ml⁻¹ doxycycline (*gray symbols*), and after induction with 2.5 ng·ml⁻¹ and pirenzepine treatment (*open symbols*). *D*, in this data set, 91% of the RoIs contained a majority of ligand treatment. *UT*, untreated.

whether including the full data set (median QB after pirenzepine, 1.47 times MEU) or only a subset of the data in which observations at receptor density levels of >80 copies· μm^{-2} were excluded from the analysis, 63.4% of the RoIs now reflected receptors dominantly in dimer/oligomer forms, a major ($p < 0.001$) increase over the untreated cells (Fig. 7*A*). To assess the effect of pirenzepine further, we examined the reversibility of the ligand-induced dimerization/oligomerization. Following treatment with pirenzepine for 90 min, the cells were washed to remove ligand from the medium, and then the degree of receptor complexity was assessed 90 min later to allow time for bound pirenzepine to dissociate from the receptors. This resulted in a dramatic reversal in the pattern of receptor complexity (Fig. 7*B*) with now only 16.2% of the hM₁-mEGFP RoIs being defined as dimeric/oligomeric, a percentage that was not different ($p > 0.05$) from that observed in sets of untreated cells that were analyzed in parallel (Fig. 7*B*).

Telenzepine is structurally closely related to pirenzepine (Fig. 1) and is also an M₁-selective antagonist. Competition binding studies using [³H]QNB and telenzepine indicated that telenzepine ($pK_i = 8.33 \pm 0.04$) displayed some 4-fold higher

affinity than pirenzepine (Fig. 8*A*). Telenzepine is also known to dissociate slowly from the M₁ receptor after binding. This feature allowed fluorophore-labeled forms of telenzepine to be used to monitor the distribution and movement of molecules of the M₁ receptor expressed in CHO cells (7). Overnight treatment with telenzepine (1 μM) of Flp-In T-Rex 293 cells induced to express hM₁-mEGFP by treatment with 100 ng·ml⁻¹ doxycycline also produced a very marked up-regulation ($p < 0.001$) of levels of the receptor as detected by both imaging the basolateral surface of the cells (Fig. 8*B*, *panels i* and *ii*) and immunoblotting studies (Fig. 8*C*). Treatment with telenzepine also enhanced quaternary structure complexity of the receptor (Fig. 8*D*) in this specific set of experiments from a very modest basal level of 7.4% of RoIs that was consistent with the receptor being in dimeric/oligomeric complexes to 60.3%. We also assessed whether an equivalent effect was produced by a more traditional, non-subtype selective muscarinic antagonist. Atropine is the prototypic muscarinic blocker and, based on competition with [³H]QNB to bind to the M₁ receptor construct (Fig. 8*A*), has high affinity for this receptor ($pK_i = 9.06 \pm 0.04$). Sustained treatment of cells induced to express hM₁-mEGFP with atro-

Antagonist Reorganization of Muscarinic Receptor Structure

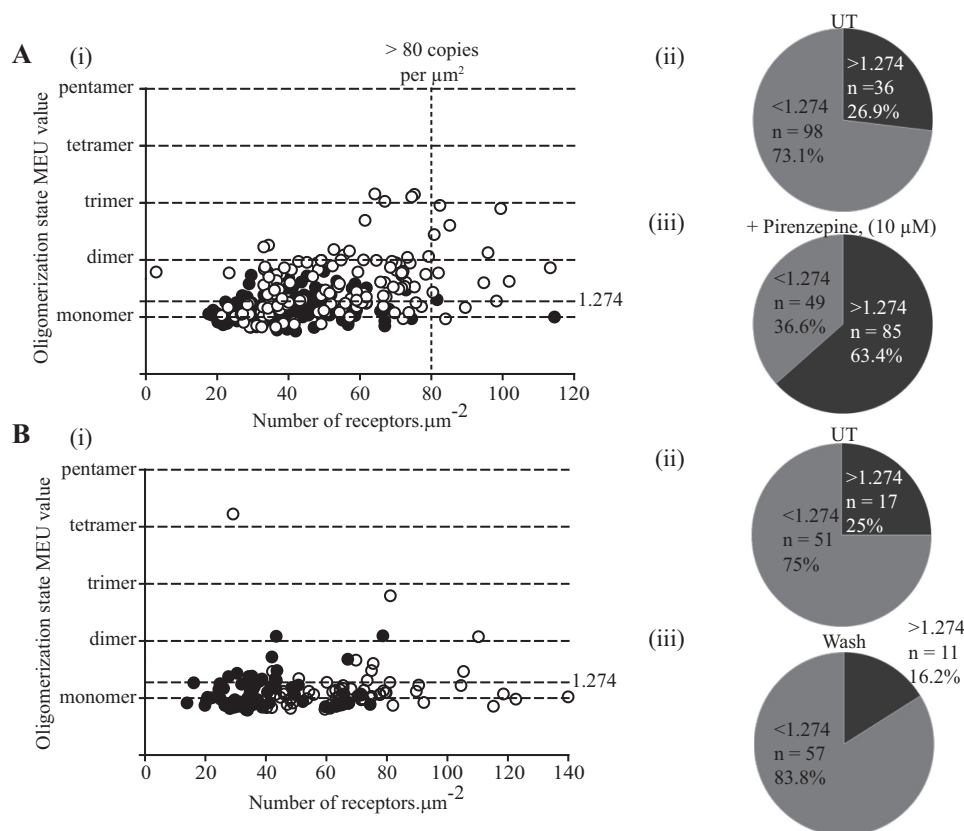


FIGURE 7. Short term treatment with pirenzepine also promotes hM₁ receptor dimer/oligomeric organization, and removal of the ligand results in reversal. Flp-In T-REx 293 cells harboring hM₁-mEGFP were treated with 100 ng·ml⁻¹ doxycycline for 24 h to induce expression of the receptor construct. *A*, cells were then treated with pirenzepine (10 μM) (open symbols) or vehicle (filled symbols) for 90 min. Pirenzepine treatment resulted in a small increase in cell surface receptor levels (54.1 ± 1.7 versus 41.8 ± 1.3 copies· μm^{-2}) (panel *i*) but a substantial increase in RoIs containing predominantly high order oligomers (63 versus 27%) (panels *ii* and *iii*). *B*, following washing of cells that had been exposed to pirenzepine (open symbols) or untreated (filled symbols), quaternary organization was assessed 90 min later (panel *i*). In this study, 25% of RoIs from the previously untreated cells were now estimated to have hM₁-mEGFP in predominantly dimeric/oligomeric forms, whereas for those previously exposed to pirenzepine this was 16% (panels *ii* and *iii*). UT, untreated.

pirenzepine (100 nM) also produced a significant ($p < 0.05$) up-regulation of the amount of the receptor construct at the basolateral surface of these cells from 31.7 ± 1.0 to 74.4 ± 4.6 receptors· μm^{-2} (Fig. 8*B*, panel *iii*), an effect that was also detected in immunoblotting studies (Fig. 8*C*). However, analysis by SpIDA showed that, in contrast with pirenzepine and telenzepine, atropine treatment did not result in an overall increase in the proportion of RoIs assessed as containing predominantly receptor dimers (Fig. 8*E*), although observation of individual RoI did suggest the presence of a small proportion of higher complexes (Fig. 8*E*). Based on this potentially surprising difference, we also explored the effects of a further muscarinic receptor subtype non-selective antagonist. We selected NMS because it is structurally related to atropine. Competition binding studies with [³H]QNB indicated NMS to bind hM₁-mEGFP with high affinity ($pK_i = 9.16 \pm 0.17$ (Fig. 8*A*). Sustained treatment of cells with NMS (50 nM) again produced a degree of up-regulation of hM₁-mEGFP levels as assessed by immunoblotting studies (Fig. 8*C*). However, as both imaging studies of the basolateral membrane (Fig. 8*B*, panel *iv*) and quantification of fluorescence intensity of imaged RoIs (Fig. 8*F*) did not demonstrate this effect, it is assumed the extra copies of the receptor detected by the immunoblotting reflect that the cellular location of these are not within the basolateral membrane. Notably,

as for atropine, sustained treatment with NMS had very limited effect on hM₁-mEGFP quaternary organization (Fig. 8*F*).

The contribution of cytoskeletal structure to hM₁-mEGFP quaternary organization was then assessed by treatment of cells induced to express hM₁-mEGFP with the actin-depolymerizing agent cytochalasin D (2.5 $\mu\text{g}\cdot\text{ml}^{-1}$; 3 h). This treatment generated a number of challenges for SpIDA. As anticipated, this treatment resulted in the cells becoming more rounded (Fig. 9*A*) and, as anticipated from this, having reduced basolateral membrane contact with the glass coverslip (Fig. 9*B*). However, following control measurements in cells induced to express the P-M-mEGFP construct and similarly treated with cytochalasin D, we were able to perform SpIDA studies (Fig. 9*C*). Treatment with cytochalasin D for this period did not up-regulate basolateral levels of hM₁-mEGFP (Fig. 9*C*) but did increase receptor quaternary structure complexity (Fig. 9*C*). Interestingly, using a very different approach, a similar observation has been made for the serotonin 5-HT_{1A} receptor (28).

Although pirenzepine and telenzepine are M₁-selective antagonists, they also can interact with other muscarinic receptor subtypes. The M₃ receptor is closely related to the M₁ subtype and also signals selectively via G_q/G₁₁ family G proteins. An M₃ muscarinic receptor construct (hM₃-mEGFP) akin to hM₁-mEGFP was generated and cloned into the Flp-In T-REx

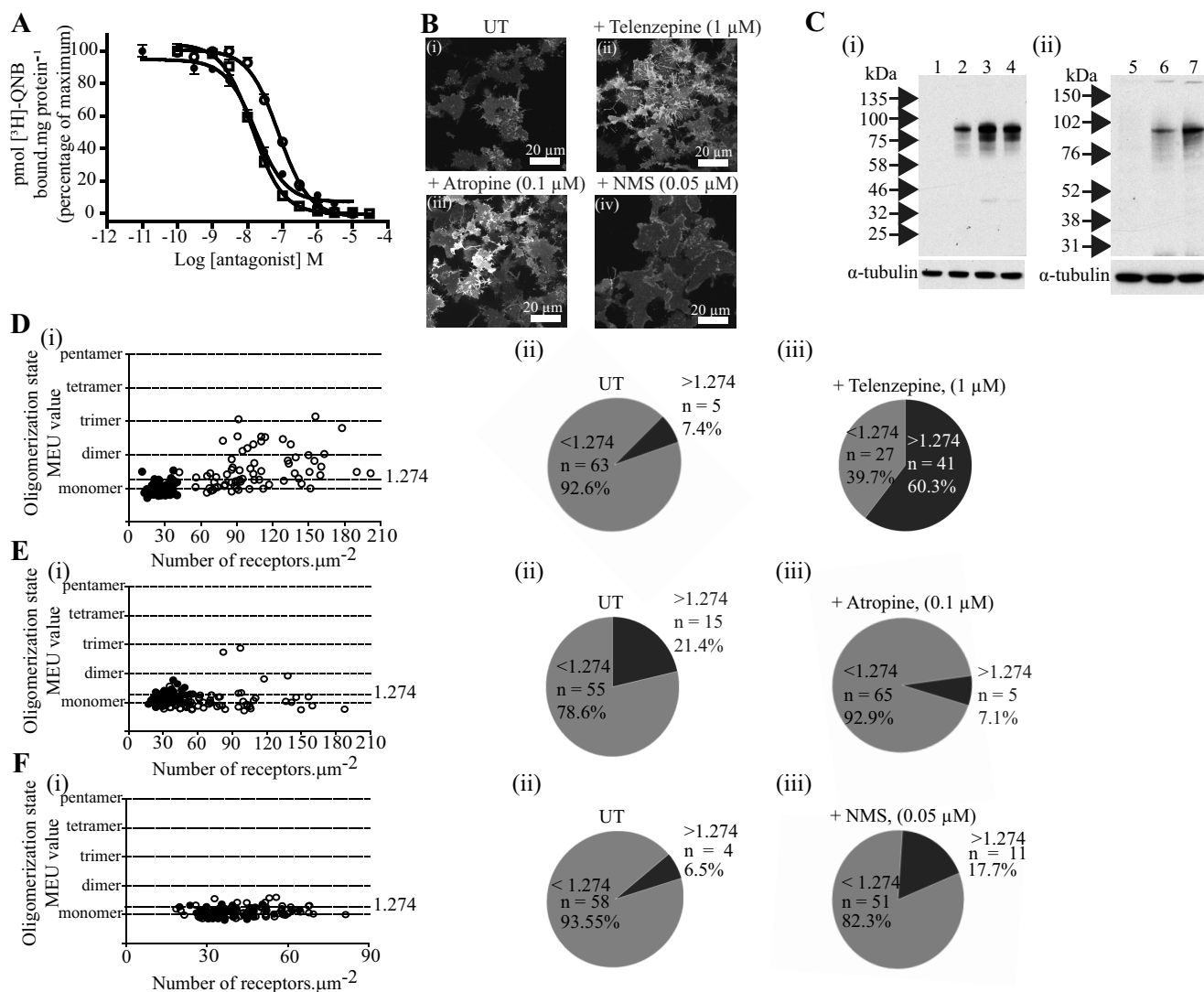


FIGURE 8. Telenzepine, but not atropine or *N*-methylscopolamine, also promotes M_1 receptor oligomerization. As in Fig. 3, cells harboring hM₁-mEGFP were treated with 100 ng·ml⁻¹ doxycycline for 24 h to induce expression of the receptor construct. *A*, membrane preparations from these cells were used in ligand binding studies using a fixed concentration of [³H]QNB (1 nM) and varying concentrations of either telenzepine (open circles), atropine (open squares), or *N*-methylscopolamine (filled circles). Shown are representative plots from $n = 3$; error bars represent \pm S.E. *B*, images of the basolateral surface of cells treated with vehicle (UT) (panel i), telenzepine (panel ii), atropine (panel iii), or NMS (panel iv). *C*, immunoblotting of cell lysates confirmed up-regulation of hM₁-mEGFP following treatment with telenzepine (panel i, lane 3), atropine (panel i, lane 4), or *N*-methylscopolamine (panel ii, lane 7). Cell lysate from uninduced cells (panel i, lane 1 and panel ii, lane 5) and from cells treated with the vehicle (panel i, lane 2 and panel ii, lane 6) were also loaded for comparison. Detection of α -tubulin acted as a loading control. *D*, *E*, and *F*, comparisons of QB (presented as monomeric equivalent units) and receptor expression levels in cells induced to express hM₁-mEGFP by treatment with 100 ng·ml⁻¹ doxycycline that were then untreated (filled symbols) or treated with 1 μM telenzepine (*D*, panel i, open symbols), 0.1 μM atropine (*E*, panel i, open symbols), or 0.05 μM *N*-methylscopolamine (*F*, panel i, open symbols) for 16 h. Although treatment with telenzepine produced a large increase in the proportion of Rols containing predominantly receptor dimers/oligomers (*D*, panels ii and iii), atropine (*E*, panels ii and iii), and *N*-methylscopolamine (*F*, panels ii and iii) did not.

locus of Flp-In T-REx 293 cells to allow doxycycline-controlled regulation of expression (Fig. 10A). The overall size of the M₃ receptor is considerably larger than the M₁ subtype, largely because of a markedly longer third intracellular loop. As such, the apparent molecular mass of this construct (approximately 140 kDa) was much greater in anti-GFP immunoblots of SDS-PAGE-resolved lysates of these cells (Fig. 10A). [³H]NMS is a high affinity muscarinic antagonist that, because it is hydrophilic and, therefore, does not easily cross the plasma membrane of intact cells, can be used to identify cell surface muscarinic receptors. Specific binding of a near saturating concentration of this ligand also confirmed doxycycline concentration-dependent expression of hM₃-mEGFP (Fig. 10B).

Confocal imaging of cells induced to express hM₃-mEGFP indicated that most of the receptor was present at the plasma membrane, in this case even without treatment with an antagonist ligand (Fig. 10C). As anticipated for a G_q/G₁₁-coupled receptor, the muscarinic agonist carbachol stimulated production of inositol phosphates in a concentration-dependent fashion in cells induced to express hM₃-mEGFP but not in cells that were not pretreated with doxycycline (Fig. 10D). Competition binding studies using [³H]QNB (K_d for hM₃-mEGFP = 0.28 ± 0.05 nM) allowed estimation of the affinity of pirenzepine ($pK_i = 5.92 \pm 0.09$), telenzepine ($pK_i = 7.15 \pm 0.02$), and atropine ($pK_i = 7.97 \pm 0.06$). Importantly, at concentrations assessed from [³H]QNB competition binding experiments to be at least

Antagonist Reorganization of Muscarinic Receptor Structure

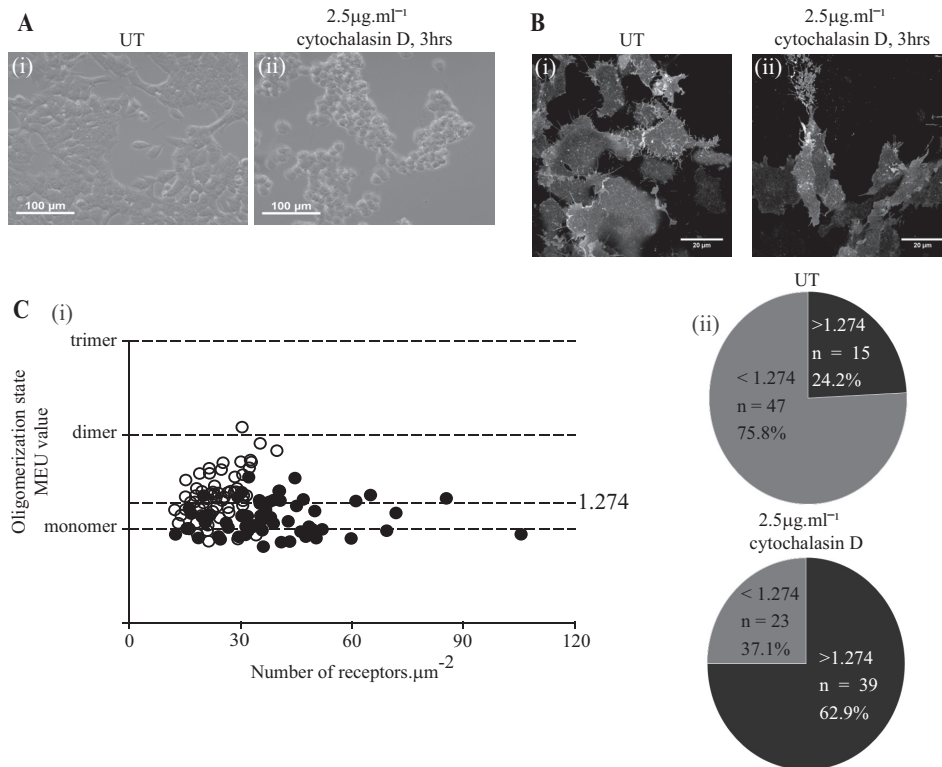


FIGURE 9. Actin cytoskeleton destabilization promotes M_1 receptor oligomerization. Flp-In T-Rex 293 cells harboring hM_1 -mEGFP were treated with doxycycline ($100 \text{ ng}\cdot\text{ml}^{-1}$) for 24 h. *A*, bright field images of cells treated with vehicle (UT) (panel *i*) or with cytochalasin D (panel *ii*). *B*, images of the basolateral surface of cells treated with vehicle (UT) (panel *i*) or cytochalasin D (panel *ii*). *C*, comparisons of QB (presented as monomeric equivalent units) and receptor expression levels in cells treated with the vehicle (panel *i*, filled symbols) or with cytochalasin D (panel *i*, open symbols) for 3 h. Treatment with cytochalasin D produced a substantial increase in the proportion of RoIs containing a high percentage of receptor dimers/oligomers (panel *ii*).

100 times K_D , each of pirenzepine ($200 \mu\text{M}$), telenzepine ($10 \mu\text{M}$), and atropine ($10 \mu\text{M}$) fully blocked carbachol-induced inositol phosphate generation (Fig. 10D). Notably, unlike the hM_1 -mEGFP construct, sustained treatment with any of these three antagonists at these concentrations failed to up-regulate levels of hM_3 -mEGFP whether assessed via immunoblotting studies performed on cell lysates (Fig. 10E) or by direct observation of the basolateral surface of the cells (Fig. 10F).

When these cells were induced to express hM_3 -mEGFP using a maximally effective concentration of doxycycline ($100 \text{ ng}\cdot\text{ml}^{-1}$), expression at the basolateral surface was measured to be $40.3 \pm 2.6 \text{ copies}\cdot\mu\text{m}^{-2}$ (Fig. 11A). The median QB corresponded to 1.08 MEU ($n = 132$) (Fig. 11B). SpIDA of the individual observations indicated that in 81.1% of the RoIs the receptor was predominantly monomeric. Analysis of RoIs following sustained treatment with each of pirenzepine, telenzepine, and atropine confirmed that these ligands did not alter the mean expression levels of hM_3 -mEGFP (Fig. 11A), and neither did they alter the QB observed (Fig. 11B). Moreover, analysis of individual observations did not support any regulation of the hM_3 receptor monomer-oligomer distribution (Fig. 11, C and D).

Discussion

Although it is well established that monomers of members of the rhodopsin-like, class A group of GPCRs can interact to generate dimers and/or higher order oligomers (1, 2), issues relating to the stability or otherwise of such interactions and how this might vary between both different receptors and in cells

and tissues expressing different amounts of an individual receptor remain unresolved. Thus, although the formyl peptide receptor 1, when present in CHO cells at rather low expression levels, has been observed to interconvert between monomers and dimers with subsecond kinetics (29) and the hM_1 receptor expressed in CHO cells has also been reported to exist as a rapidly interconverting mixture of monomers and dimers (7), the technical approaches used in these studies rely on and require low level expression. At the other extreme, concerns have been raised over the possibility that certain studies on the organizational structure of class A GPCRs have used high level receptor "overexpression" that might have produced outcomes in terms of receptor-receptor interactions that are not of physiological relevance (1, 2). However, it is important to note that, particularly in the CNS, ligand binding studies performed on membranes generated from bulk tissue have indicated that receptors such as the M_1 muscarinic receptor are expressed, in striatum for example, at levels of at least $1 \text{ pmol}\cdot\text{mg}$ of membrane protein⁻¹ (15), and this is presumably higher in cells that actually express the receptor, whereas other GPCRs, including cannabinoid and opioid receptors, are expressed regionally at significantly higher levels. It has also been suggested that receptor organizational complexity may increase with expression levels. Indeed, Calebiro *et al.* (30) observed just such a relationship for both the β_1 - and β_2 -adrenoceptors following expression in HEK293 cells and were able to detect increasing proportions of both dimers and oligomers of each receptor. Equally, a

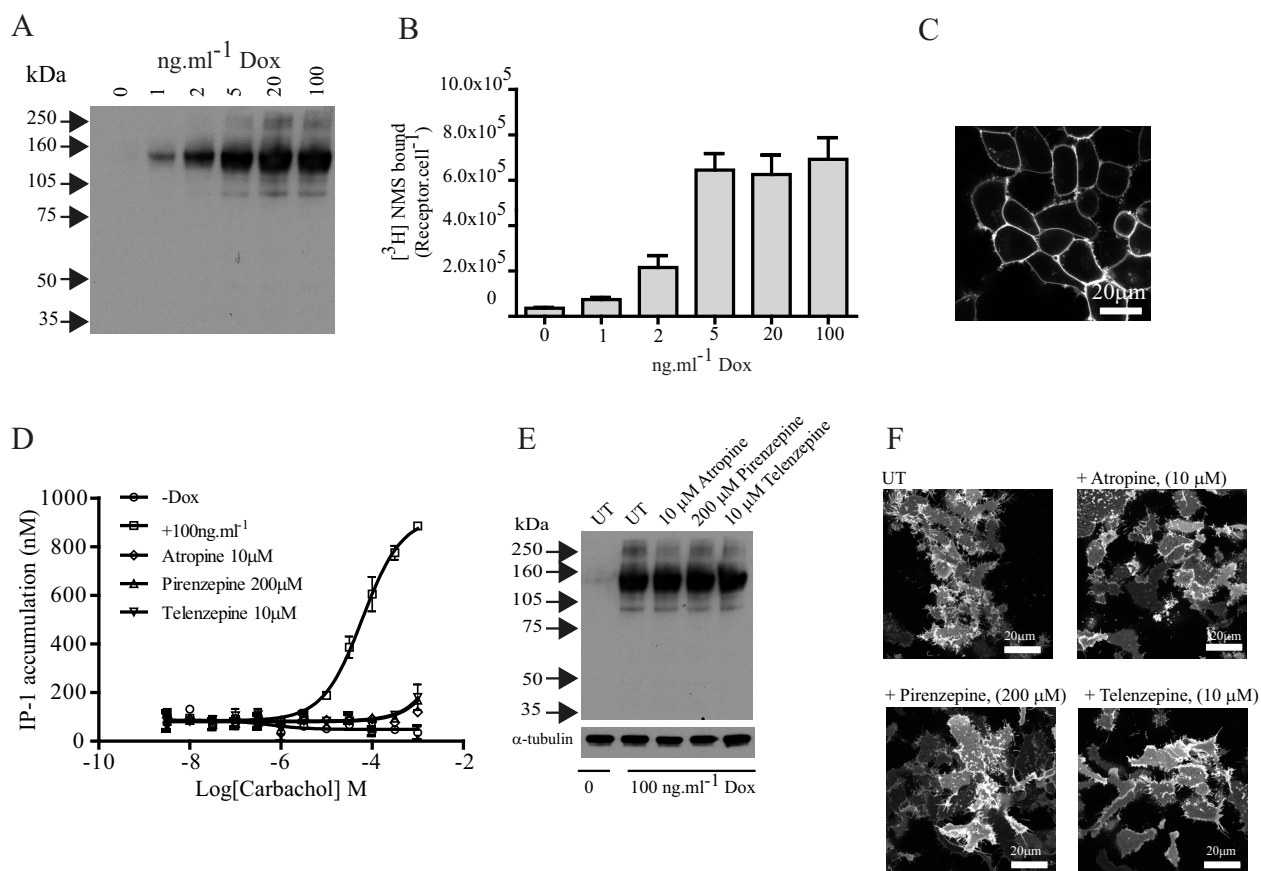


FIGURE 10. **Muscarinic antagonists do not up-regulate levels of the M_3 receptor.** Flp-In T-Rex 293 cells harboring hM_3 -mEGFP were treated with the indicated concentrations of doxycycline (Dox) for 24 h to induce expression of the receptor construct. *A*, anti-GFP immunoblotting of cell lysates detected hM_3 -mEGFP as a 140-kDa polypeptide. *B*, specific binding of [3 H]NMS confirmed that the level of expression of hM_3 -mEGFP at the surface of intact cells is dependent on doxycycline concentration. Shown are combined data from $n = 3$ experiments; error bars represent \pm S.E. *C*, confocal image of cells induced to express hM_3 -mEGFP shows it to be restricted to the plasma membrane. *D*, the ability of the muscarinic agonist carbachol to promote generation of inositol monophosphates in these cells is dependent upon treatment with doxycycline (compare $-Dox$ and $100 \text{ ng}\cdot\text{ml}^{-1}$) and is fully blocked by the indicated concentrations of each of atropine, pirenzepine, and telenzepine. Shown are representative plots from $n = 3$; error bars represent \pm S.E. *E* and *F*, sustained treatment with atropine, pirenzepine, or telenzepine does not up-regulate levels of hM_3 -mEGFP. *E*, anti-GFP immunoblotting was performed on SDS-PAGE-resolved lysates from cells not induced with doxycycline or induced to express hM_3 -mEGFP and then treated for 16 h with the indicated concentration of atropine, pirenzepine, or telenzepine. Detection of α -tubulin acted as a loading control. *F*, images of the basolateral surface of such cells. Scale bar, $20 \mu\text{m}$. UT, untreated.

similar relationship between receptor expression level and quaternary complexity has also been observed for the serotonin 5-HT_{2C} receptor (24). As such, based solely on mass action, then in a number of natively expressing systems, GPCRs may potentially be at least partially dimeric and/or oligomeric. However, it is important to note that others have suggested more stable oligomeric organization over a significant range of expression levels. For example, Herrick-Davis *et al.* (5) have indicated that over a 10-fold range of expression, between 26,000 and 260,000 copies per cell, the M_1 receptor expressed in HEK293 cells is consistently dimeric, and Guo *et al.* (31) suggested that over a 100-fold range of expression levels dopamine D_2 receptors had cross-linking characteristics consistent with them forming and remaining as tetramers. This, however, is in contrast to other studies of the dopamine D_2 receptor suggesting that "dimeric" interactions might, at best, be transient (32). Moreover, although at odds with earlier studies indicating that the serotonin 5-HT_{2C} receptor is also dimeric when expressed in HEK293 cells (33) and indeed is also reportedly dimeric in epithelial cells from choroid plexus where endogenous expression was estimated to be $32 \text{ receptors}\cdot\mu\text{m}^{-2}$ on the apical sur-

face (34), Ward *et al.* (24) noted that at expression levels above $100 \text{ receptors}\cdot\mu\text{m}^{-2}$ on the basolateral surface of HEK293 cells much of the 5-HT_{2C} receptor was present within higher order oligomers rather than dimers and that at expression levels below $50 \text{ receptors}\cdot\mu\text{m}^{-2}$ a significant proportion of this receptor was monomeric.

Herein we note in the basal state and at moderate expression levels in HEK293 cells that, although the larger proportion of the hM_1 receptor is monomeric, there is a clear fraction of dimeric forms. Moreover, treatment of the cells with the muscarinic M_1 receptor-selective antagonist pirenzepine resulted in a substantial increase in the proportion of dimeric, as well as oligomeric, forms. This is interesting from three distinct perspectives. First, these results are in agreement with those of Ilien *et al.* (26), who, by using two-photon fluorescence correlation spectroscopy in cells expressing an N-terminally fluorescent protein-tagged variant of the hM_1 receptor, were able to observe a rapid, pirenzepine-induced transition from a situation in which the receptor was predominantly monomeric to a mixture of monomers and dimers. Second, although sustained treatment of cells with pirenzepine produced a marked up-reg-

Antagonist Reorganization of Muscarinic Receptor Structure

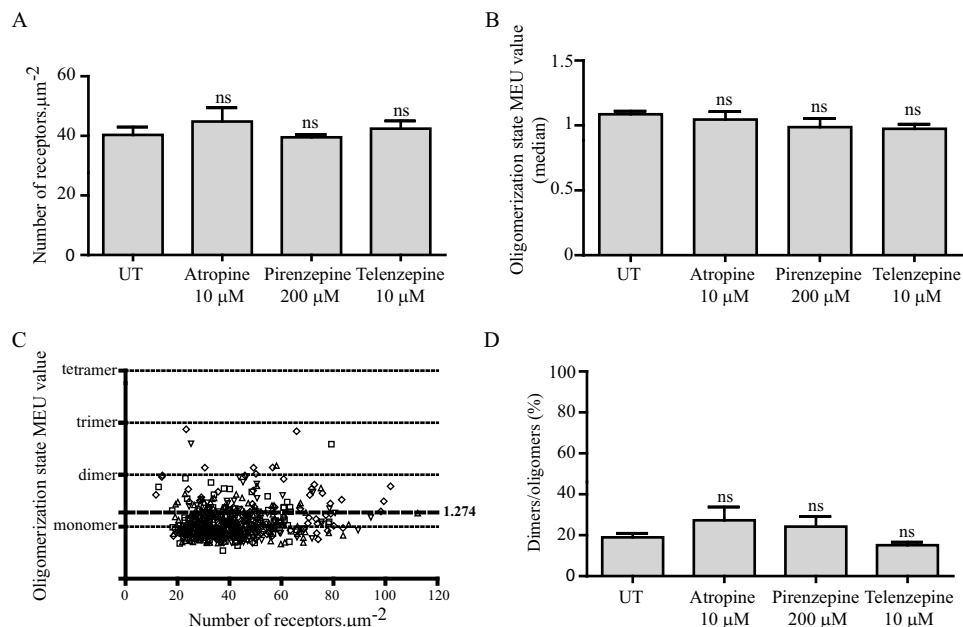


FIGURE 11. Muscarinic antagonists do not affect the quaternary organization of the M_3 receptor. Cells, as in Fig. 9, that had been induced to express hM₃-mEGFP were treated with the indicated concentrations of atropine, pirenzepine, or telenzepine for 16 h. Imaging of Rol within the basolateral surface indicated that treatment with the ligands did not alter the mean receptor expression level (A) or the overall organizational state of the receptor (B). Data are presented as monomeric equivalent units. C, full data set of individual QB values (again expressed as monomeric equivalent units) for untreated cells (squares) and those treated with atropine (diamonds), pirenzepine (triangles), or telenzepine (inverted triangles). D, assessment of percentage of Rol containing predominantly dimers/oligomers following each treatment. ns, not significantly different from untreated. All graphs show combined data from at least $n = 3$ experiments; error bars represent \pm S.E. UT, untreated.

ulation of the basolateral levels of hM₁ receptor that might have confounded interpretation of the effect of the antagonist, this concern was overcome by having the receptor expressed from a doxycycline-regulated locus whereby we were able to define conditions in which the number of receptors after sustained treatment with pirenzepine was not different from vehicle-treated cells. In this situation, there was also clearly a much greater proportion of hM₁ dimers detected after pirenzepine treatment. This demonstrated explicitly that although pirenzepine treatment does up-regulate levels of the receptor, which inherently increases the proportion of receptor dimers/oligomers, it also stabilizes receptor dimers in a manner-independent from this. It is also important to note that for the P-M-mEGFP construct, at levels well above those used to study the muscarinic receptors, this polypeptide was identified exclusively as being monomeric. Therefore, simple aspects of proximity at the levels of expression used for the hM₁ did not result in artifactual identification of apparently dimeric species. Third and perhaps most intriguingly, pirenzepine is structurally very closely related to telenzepine. A fluorophore-tagged form of telenzepine was used by Hern *et al.* (7) to label M₁ receptors for total internal reflection microscopy studies that allowed tracking and analysis of receptor monomers and dimers. As we note herein, as for the fluorescent form of telenzepine, which was used at high receptor occupancy by Hern *et al.* (7), native telenzepine caused both substantial up-regulation of the hM₁ receptor and promoted the presence of dimers. As such it is likely that Hern *et al.* (7) may have inadvertently generated a greater proportion of receptor dimers simply by their choice of fluorescent antagonist. A further fascinating feature of the studies with pirenzepine and telenzepine was that the effect of these ligands

was not mimicked by the structurally distinct muscarinic antagonists atropine and NMS. Further studies will be required to unravel the molecular basis for these differences. One potential confounding issue for these studies would have been whether addition of pirenzepine and telenzepine altered the spectral characteristics of mEGFP. We tested this directly and observed no effect.

A further key point from these studies is that the effect of pirenzepine was reversible. Following removal of the ligand, the M₁ receptor population returned to being predominantly monomeric. Although this is clearly the case, it was not realistic to accurately define the time course of this process. This reflects that, as a relatively high affinity antagonist for the hM₁ receptor, pirenzepine has a significant residency time on the receptor. As such, simply washing cells to remove bulk ligand from the medium does not intrinsically remove the ligand from the receptor. Indeed, the slow dissociation rate of telenzepine from the M₁ receptor was a key reason for Hern *et al.* (7) to select a fluorescent variant of telenzepine for their receptor tracking studies. Identification of a ligand that mimics the capacity of pirenzepine to promote M₁ receptor dimerization but has rapid “off”-rate binding kinetics will be required, therefore, to start to define the true rate of hysteresis of M₁ receptor quaternary complexes back to monomers in the absence of ligand.

Integral to the studies we have performed, SpIDA has been shown previously to be able to observe and quantify ligand-induced alterations in quaternary structure and organization of various classes of transmembrane receptor proteins. For example, using this method, we have shown that addition of epidermal growth factor results in rapid and ligand concentration-dependent dimerization of the epidermal growth factor receptor

(24). Moreover, although SpIDA demonstrated the single transmembrane domain axonal guidance receptor Robo-1 to exist basally as a dimer and that this organization was unaffected by addition of the ligand Slit-2 (25), in terms of GPCRs, higher order oligomers and even dimers of the serotonin 5-HT_{2C} receptor were pushed toward monomeric organization upon binding of antagonist ligands from two distinct chemotypes (24). Furthermore, washing of the cells to remove bulk ligand from the medium allowed a time-dependent hysteresis of quaternary complexity back toward the basal state (24). Interestingly, ligand effects on receptor quaternary organization are clearly rather selective. The M₃ muscarinic receptor is closely related to the M₁ receptor and can also bind pirenzepine although with somewhat lower affinity. Pirenzepine did not produce an equivalent effect on the M₃ receptor, however, even when the ligand was present at concentrations sufficient to fully occupy the M₃ receptor population. The molecular basis for this distinction will require many further studies, including potentially the generation of receptor point mutants and chimeras between these subtypes.

The current studies highlight that the quaternary organization of class A GPCRs can indeed be regulated by ligand binding. Given that pirenzepine and telenzepine enhance this complexity for the hM₁ receptor, whereas a group of antagonists decreased complexity of the serotonin 5-HT_{2C} receptor (24), then it will be important to explore this issue for other GPCRs in a systematic manner to begin to understand the molecular basis for these observations. Although in certain GPCRs a single transmembrane domain appears to provide a key symmetrical interface for receptor dimerization, *e.g.* transmembrane domain IV of the secretin receptor (35), studies on many GPCRs have concluded that multiple regions contribute (8, 11, 36). This has resulted in suggestions that there may be multiple ways in which receptor dimers can form, and the stability of these distinct forms may well differ (8, 37, 38). Moreover, there are suggestions, based particularly on receptor cross-linking studies, that ligands with different functionalities, *e.g.* agonists *versus* inverse agonists (39), alter details of the organization of receptor-receptor interfaces. This might well be anticipated to modify the affinity of interaction between the individual protomers and, therefore, the balance of observed quaternary structures. Clearly this is speculative, but as various mutations also alter the effectiveness of receptor dimerization and oligomerization (35–36) it would be likely that ligand effects at such mutants might be further amplified. These topics will form the basis of future studies.

Author Contributions—G. M. conceived and coordinated the study and, with the assistance of all others, wrote the paper. J. D. P. and R. J. W. designed, performed, and analyzed the experiments shown in Figs. 2–9. S. M. designed, performed, and analyzed the experiments shown in Figs. 1, 8, 10, and 11. A. G. G. provided key insights into the SpIDA. All authors reviewed the results and approved the final version of the manuscript.

References

1. Milligan, G. (2013) The prevalence, maintenance and relevance of G protein-coupled receptor oligomerization. *Mol. Pharmacol.* **84**, 158–169
2. Ferré, S., Casadó, V., Devi, L. A., Filizola, M., Jockers, R., Lohse, M. J., Milligan, G., Pin, J. P., and Guitart, X. (2014) G protein-coupled receptor oligomerization revisited: functional and pharmacological perspectives. *Pharmacol. Rev.* **66**, 413–434
3. Wess, J. (1996) Molecular biology of muscarinic acetylcholine receptors. *Crit. Rev. Neurobiol.* **10**, 69–99
4. Nenashva, T. A., Neary, M., Mashanov, G. I., Birdsall, N. J., Breckenridge, R. A., and Molloy, J. E. (2013) Abundance, distribution, mobility and oligomeric state of M₂ muscarinic acetylcholine receptors in live cardiac muscle. *J. Mol. Cell. Cardiol.* **57**, 129–136
5. Herrick-Davis, K., Grinde, E., Cowan, A., and Mazurkiewicz, J. E. (2013) Fluorescence correlation spectroscopy analysis of serotonin, adrenergic, muscarinic, and dopamine receptor dimerization: the oligomer number puzzle. *Mol. Pharmacol.* **84**, 630–642
6. Redka, D. S., Morizumi, T., Elmslie, G., Paranthaman, P., Shivnaraine, R. V., Ellis, J., Ernst, O. P., and Wells, J. W. (2014) Coupling of G proteins to reconstituted monomers and tetramers of the M₂ muscarinic receptor. *J. Biol. Chem.* **289**, 24347–24365
7. Hern, J. A., Baig, A. H., Mashanov, G. I., Birdsall, B., Corrie, J. E., Lazareno, S., Molloy, J. E., and Birdsall, N. J. (2010) Formation and dissociation of M₁ muscarinic receptor dimers seen by total internal reflection fluorescence imaging of single molecules. *Proc. Natl. Acad. Sci. U.S.A.* **107**, 2693–2698
8. McMillin, S. M., Heusel, M., Liu, T., Costanzi, S., and Wess, J. (2011) Structural basis of M₃ muscarinic receptor dimer/oligomer formation. *J. Biol. Chem.* **286**, 28584–28598
9. Hu, J., Thor, D., Zhou, Y., Liu, T., Wang, Y., McMillin, S. M., Mistry, R., Challiss R. A., Costanzi, S., and Wess, J. (2012) Structural aspects of M₃ muscarinic acetylcholine receptor dimer formation and activation. *FASEB J.* **26**, 604–616
10. Patowary, S., Alvarez-Curto, E., Xu, T. R., Holz, J. D., Oliver, J. A., Milligan, G., and Raicu, V. (2013) The muscarinic M₃ acetylcholine receptor exists as two differently sized complexes at the plasma membrane. *Biochem. J.* **452**, 303–312
11. Liste, M. J., Caltabiano, G., Ward, R. J., Alvarez-Curto, E., Marsango, S., and Milligan, G. (2015) The molecular basis of oligomeric organization of the human M₃ muscarinic acetylcholine receptor. *Mol. Pharmacol.* **87**, 936–953
12. Goin, J. C., and Nathanson, N. M. (2006) Quantitative analysis of muscarinic acetylcholine receptor homo- and heterodimerization in live cells: regulation of receptor down-regulation by heterodimerization. *J. Biol. Chem.* **281**, 5416–5425
13. Aslanoglou, D., Alvarez-Curto, E., Marsango, S., and Milligan, G. (2015) Distinct agonist regulation of muscarinic acetylcholine M₂-M₃ heteromers and their corresponding homomers. *J. Biol. Chem.* **290**, 14785–14796
14. Alvarez-Curto, E., Ward, R. J., Pediani, J. D., and Milligan, G. (2010) Ligand regulation of the quaternary organization of cell surface M₃ muscarinic acetylcholine receptors analyzed by fluorescence resonance energy transfer (FRET) imaging and homogeneous time-resolved FRET. *J. Biol. Chem.* **285**, 23318–23330
15. Hammer, R., Berrie, C. P., Birdsall, N. J., Burgen, A. S., and Hulme, E. C. (1980) Pirenzepine distinguishes between different subclasses of muscarinic receptors. *Nature* **283**, 90–92
16. Alvarez-Curto, E., Pediani, J. D., and Milligan, G. (2010) Applications of fluorescence and bioluminescence resonance energy transfer to drug discovery at G protein coupled receptors. *Anal. Bioanal. Chem.* **398**, 167–180
17. Marsango, S., Varela, M. J., and Milligan, G. (2015) Approaches to characterize and quantify oligomerization of GPCRs. *Methods Mol. Biol.* **1335**, 95–105
18. Godin, A. G., Costantino, S., Lorenzo, L. E., Swift, J. L., Sergeev, M., Ribeiro-da-Silva, A., De Koninck, Y., and Wiseman, P. W. (2011) Revealing protein oligomerization and densities *in situ* using spatial intensity distribution analysis. *Proc. Natl. Acad. Sci. U.S.A.* **108**, 7010–7015
19. Barbeau, A., Godin, A. G., Swift, J. L., De Koninck, Y., Wiseman, P. W., and Beaulieu, J. M. (2013) Quantification of receptor tyrosine kinase activation and transactivation by G-protein-coupled receptors using spatial intensity distribution analysis (SpIDA). *Methods Enzymol.* **522**, 109–131

Antagonist Reorganization of Muscarinic Receptor Structure

20. Swift, J. L., Godin, A. G., Doré, K., Freland, L., Bouchard, N., Nimmo, C., Sergeev, M., De Koninck, Y., Wiseman, P. W., and Beaulieu, J. M. (2011) Quantification of receptor tyrosine kinase transactivation through direct dimerization and surface density measurements in single cells. *Proc. Natl. Acad. Sci. U.S.A.* **108**, 7016–7021
21. Godin, A. G., Rappaz, B., Potvin-Trottier, L., Kennedy, T. E., De Koninck, Y., and Wiseman, P. W. (2015) Spatial intensity distribution analysis reveals abnormal oligomerization of proteins in single cells. *Biophys. J.* **109**, 710–721
22. von Stetten, D., Noirclerc-Savoye, M., Goedhart, J., Gadella, T. W., Jr., and Royant, A. (2012) Structure of a fluorescent protein from *Aequorea victoria* bearing the obligate-monomer mutation A206K. *Acta Crystallogr. Sect. F Struct. Biol. Cryst. Commun.* **68**, 878–882
23. Zacharias, D. A., Violin, J. D., Newton, A. C., and Tsien, R. Y. (2002) Partitioning of lipid-modified monomeric GFPs into membrane microdomains of live cells. *Science* **296**, 913–916
24. Ward, R. J., Pediani, J. D., Godin, A. G., and Milligan, G. (2015) Regulation of oligomeric organization of the serotonin 5-hydroxytryptamine 2C (5-HT_{2C}) receptor observed by spatial intensity distribution analysis. *J. Biol. Chem.* **290**, 12844–12857
25. Zakrys, L., Ward, R. J., Pediani, J. D., Godin, A. G., Graham, G. J., and Milligan, G. (2014) Roundabout 1 exists predominantly as a basal dimeric complex and this is unaffected by binding of the ligand Slit2. *Biochem. J.* **461**, 61–73
26. Ilien, B., Glasser, N., Clamme, J. P., Didier, P., Piemont, E., Chinnappan, R., Daval, S. B., Galzi, J. L., and Mely, Y. (2009) Pirenzepine promotes the dimerization of muscarinic M1 receptors through a three-step binding process. *J. Biol. Chem.* **284**, 19533–19543
27. Ward, R. J., Alvarez-Curto, E., and Milligan, G. (2011) Using the Flp-InTM T-RexTM system to regulate GPCR expression. *Methods Mol. Biol.* **746**, 21–37
28. Ganguly, S., Clayton, A. H., and Chattopadhyay, A. (2011) Organization of higher-order oligomers of the serotonin_{1A} receptor explored utilizing homo-FRET in live cells. *Biophys. J.* **100**, 361–368
29. Kasai, R. S., Suzuki, K. G., Prossnitz, E. R., Koyama-Honda, I., Nakada, C., Fujiwara, T. K., and Kusumi, A. (2011) A. Full characterization of GPCR monomer-dimer dynamic equilibrium by single molecule imaging. *J. Cell Biol.* **192**, 463–480
30. Calebiro, D., Rieken, F., Wagner, J., Sungkaworn, T., Zabel, U., Borzi, A., Cocucci, E., Zürn, A., and Lohse, M. J. (2013) Single-molecule analysis of fluorescently labeled G-protein-coupled receptors reveals complexes with distinct dynamics and organization. *Proc. Natl. Acad. Sci. U.S.A.* **110**, 743–748
31. Guo, W., Urizar, E., Kralikova, M., Mobarec, J. C., Shi, L., Filizola, M., and Javitch, J. A. (2008) Dopamine D2 receptors form higher order oligomers at physiological expression levels. *EMBO J.* **27**, 2293–2304
32. Fonseca, J. M., and Lambert, N. A. (2009) Instability of a class A G protein-coupled receptor oligomer interface. *Mol. Pharmacol.* **75**, 1296–1299
33. Herrick-Davis, K., Grinde, E., Lindsley, T., Cowan, A., and Mazurkiewicz, J. E. (2012) Oligomer size of the serotonin 5-hydroxytryptamine 2C (5-HT_{2C}) receptor revealed by fluorescence correlation spectroscopy with photon counting histogram analysis: evidence for homodimers without monomers or tetramers. *J. Biol. Chem.* **287**, 23604–23614
34. Herrick-Davis, K., Grinde, E., Lindsley, T., Teitler, M., Mancía, F., Cowan, A., and Mazurkiewicz, J. E. (2015) Native serotonin 5-HT_{2C} receptors are expressed as homodimers on the apical surface of choroid plexus epithelial cells. *Mol. Pharmacol.* **87**, 660–673
35. Harikumar, K. G., Pinon, D. I., and Miller, L. J. (2007) Transmembrane segment IV contributes a functionally important interface for oligomerization of the class II G protein-coupled secretin receptor. *J. Biol. Chem.* **282**, 30363–30372
36. Marsango, S., Caltabiano, G., Pou, C., Varela Liste, M. J., and Milligan, G. (2015) Analysis of human dopamine D3 receptor quaternary structure. *J. Biol. Chem.* **290**, 15146–15162
37. Johnston, J. M., Wang, H., Provasi, D., and Filizola, M. (2012) Assessing the relative stability of dimer interfaces in G protein-coupled receptors. *PLoS Comput. Biol.* **8**, e1002649
38. Jastrzebska, B., Chen, Y., Orban, T., Jin, H., Hofmann, L., and Palczewski, K. (2015) Disruption of rhodopsin dimerization with synthetic peptides targeting an interaction interface. *J. Biol. Chem.* **290**, 25728–25744
39. Guo, W., Shi, L., Filizola, M., Weinstein, H., and Javitch, J. A. (2005) Crosstalk in G protein-coupled receptors: changes at the transmembrane homodimer interface determine activation. *Proc. Natl. Acad. Sci. U.S.A.* **102**, 17495–17500